

Methane hydrate under high pressure

Toshiaki Iitaka* and Toshikazu Ebisuzaki

Computational Astrophysics Laboratory, RIKEN (The Institute of Physical and Chemical Research) 2-1 Hirosawa, Wako, Saitama 351-0198, Japan

(Received 12 May 2003; revised manuscript received 11 September 2003; published 14 November 2003)

The structural, electronic, and spectroscopic properties of a high-pressure phase of methane hydrate are studied by first-principles electronic structure calculations. A detailed analysis of the atomic positions suggests that *ionization* of hydrogen-bonded water molecules occurs around 40 GPa and *centering* or symmetrization of hydrogen bonds occurs around 70 GPa. These pressures are much lower compared to ionization around 55 GPa and centering around 100 GPa in pure ice. The transition may be observed with low-temperature IR/Raman spectroscopy of OH stretching modes, neutron diffraction, or $^1\text{H-NMR}$.

DOI: 10.1103/PhysRevB.68.172105

PACS number(s): 62.50.+p, 82.75.-z, 71.15.Pd

Methane hydrate (MH), known as *burning ice*, is a special class of ice that contains methane molecules in cages or networks of hydrogen-bonded water molecules. Low-pressure phase of methane hydrate (MH-I) forms sI structure of cages.¹ MH-I, abundant in the deep ocean, has been attracting attention of the industry as a key energy resource, whose amount is estimated twice as much as the total fossil-fuel reserve.¹

MH is also known as an important material for understanding the mystery of the atmosphere of Titan, the largest satellite of Saturn. The conventional theory² could not explain abundant methane gas in Titan's atmosphere because MH-I inside Titan was assumed to decompose into ice and methane around 1 or 2 GPa, and escape to the atmosphere to be photodecomposed in the early stage of Titan's history. To understand this mystery is one of the goals of the Cassini-Huygens spacecraft, which started its journey in 1997 and will arrive at Saturn system in 2004.³

On the Earth, in 2001, Loveday *et al.*^{4,5} discovered new phases of MH by x-ray and neutron diffraction experiments under high pressure: MH-I transforms to MH-II (sH cage structure) at 1 GPa, and then to MH-III phase (orthorhombic filled ice structure) at 2 GPa, which survives at least up to 10 GPa. Other researchers reported similar high-pressure phases.^{6,7} Recently Hirai *et al.*⁸ reported that MH-III survives up to 42 GPa at room temperature. Shimizu *et al.*⁹ have measured the site and pressure dependences of CH- and OH-vibration frequencies in these phases up to 5.2 GPa. Discovery of these high-pressure phases offers us a new explanation of abundant methane gas in Titan's atmosphere: methane gas may be reserved in thick layers of MH-III under Titan's surface and gradually emitted to the atmosphere from the reservoir.⁴

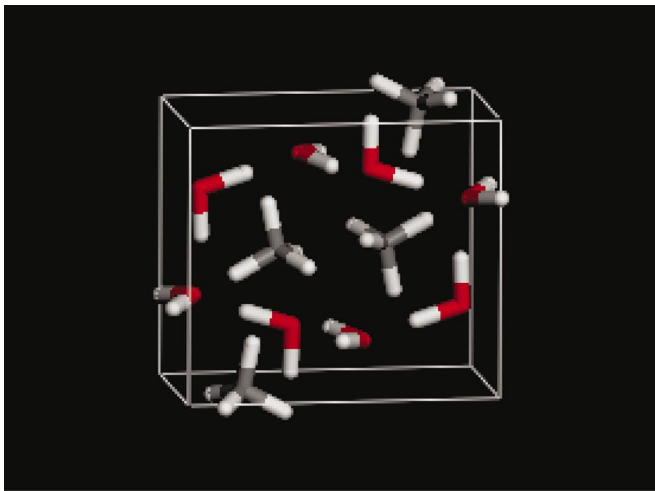
In this paper, we focus on the features of MH-III as a promising material for investigating *centering* or symmetrization of hydrogen bonds between water molecules. In spite of a long quest to understand this phenomenon,¹⁰⁻²⁰ a unified theoretical explanation of various experimental results appeared only recently,¹² partly because of difficulties in measurements under very high pressures. Advantage of using MH-III for studying the centering is that it is expected to occur at a much lower pressure (70 GPa) than that of pure ice (ice VII-ice X transition around 100 GPa),

which may make the difficult high-pressure experiments easier. In the following, we calculate the crystal structure and vibrational spectra of MH-III by using the density-functional theory, so that we can predict and analyze experimental results.

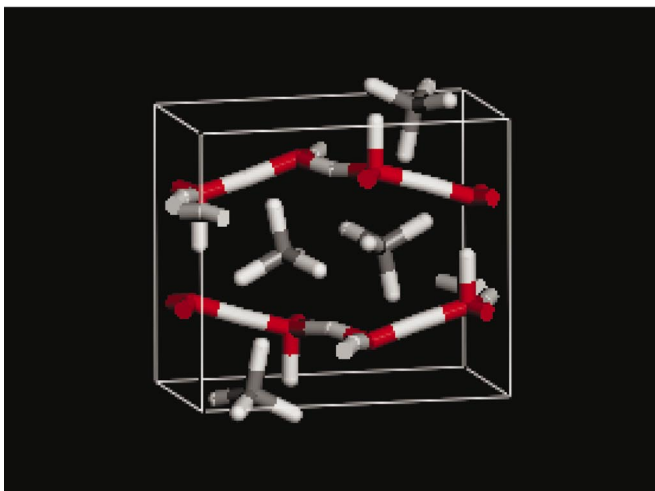
We modeled the crystal structure of MH-III at 3 GPa by using the *Pm \bar{c} n* symmetry, the lattice parameters and the position of atoms determined by the diffraction experiment.⁵ We chose the orientation of methane molecules carefully so that the molecules become close packed. The model consists of four methane and eight water molecules in the unit cell, of which one methane and two water molecules are symmetrically inequivalent. This structure was found stable after full geometrical optimization, in which the enthalpy $H=E+PV$ was minimized by varying the lattice vectors and the positions of atoms without any constraints such as crystal symmetry. The structures at higher pressures (Fig. 1) were calculated in a similar manner.

The details of the electronic structure calculation²¹ are as follows: the valence wave functions are expanded in a plane wave basis set truncated at a kinetic energy of 1520 eV. The electron-ion interactions are described by the Vanderbilt-type ultrasoft pseudopotentials.²² The effects of exchange-correlation interaction are treated within the generalized gradient approximation of Perdew *et al.*²³ The Brillouin zones are sampled with $4\times 2\times 2$ Monkhorst-Pack k points²⁴ by using time-reversal symmetry only. Convergence was checked with respect to cutoff energy and number of k points. Increasing cutoff energy to 3040 eV changed the total energy 15 meV per atom, and increasing the number of k points to 48 changed only 0.03 meV per atom. In the geometrical optimization, the total stress tensor is reduced to the order of 0.01 GPa by using the finite basis-set corrections.²⁵

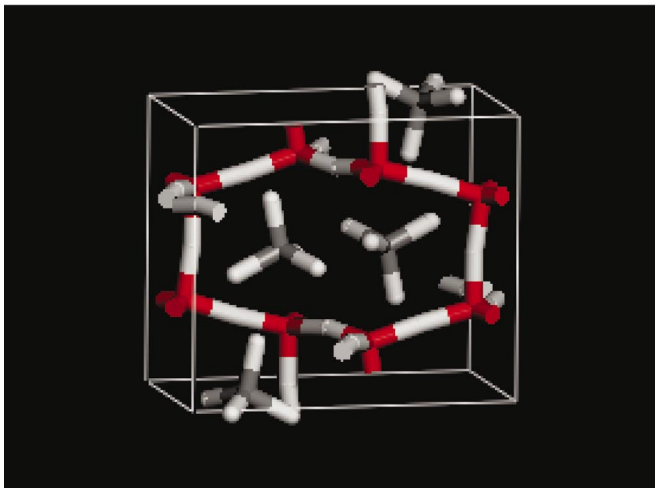
Figure 2 shows the pressure dependence of the calculated lattice parameters at zero temperature. It agrees well with the experimental data at room temperature by Hirai *et al.*⁸ The cell is most soft along the c axis. This feature is also evident from Fig. 1. The compression of the cell along the c axis is mainly caused by the flattening of the two graphite like wrinkled sheets normal to c axis. As a result, the hydrogen-bond network at very high pressures becomes sp_2 -like structure in contrast to sp_3 structure of ice Ih.



(a)



(b)



(c)

FIG. 1. (Color) Crystal structure of MH-III (a) 40 GPa, (b) 60 GPa, and (c) 80 GPa.

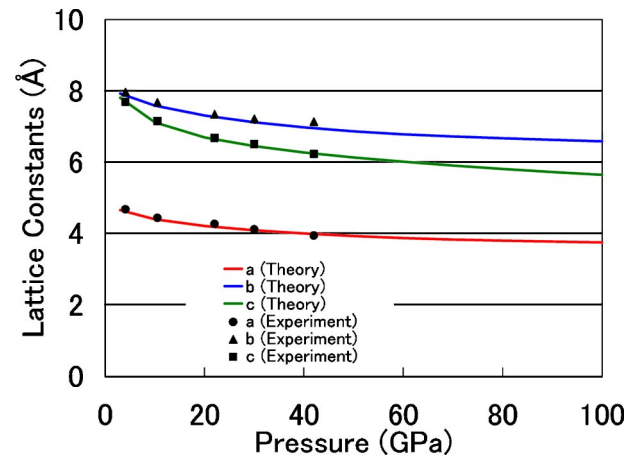


FIG. 2. (Color online) Lattice parameters: The solid lines indicate the present density-functional-theory calculation. The symbols indicate the experimental results of Hirai *et al.* (Ref. 8).

In pure ice, centering of the hydrogen bond $\text{O}-\text{H}\cdots\text{O}$ occurs as the oxygen-oxygen distance $d(\text{OO})$ of two hydrogen-bonded water molecules decreases with pressure increase.^{10,11} At large $d(\text{OO})$ the proton occupies one of the two potential minima along the $\text{O}-\text{H}\cdots\text{O}$ bond. As $d(\text{OO})$ becomes smaller the barrier between the two minima becomes lower. When $d(\text{OO})$ becomes smaller than some critical distance, the proton occupies the single minimum at the midpoint between the two oxygen atoms (centering). In the following, we neglect the effect of finite temperature and quantum nature of hydrogen atom unless otherwise stated. Figure 3 shows $d(\text{OO})$ as a function of pressure. There are three curves corresponding to the three symmetrically inequivalent $\text{O}-\text{H}\cdots\text{O}$ bonds. Around 70 GPa $d(\text{OO})$'s become as short as the hydrogen bond centering occurs in pure ice.¹² Indeed, Fig. 1 shows that the centering occurs around this pressure. Figure 4 shows the ratio $d(\text{OH})/d(\text{OO})$ as a function of pressure. The ratio starts from 0.35 (water molecule) at 3 GPa and reaches to 0.5 (centering) around 70 GPa.

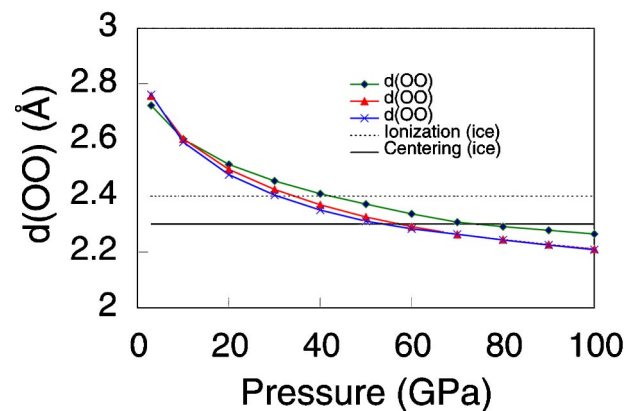


FIG. 3. (Color online) Three symmetrically different distances between oxygen atoms, $d(\text{OO})$, as a function of pressure: the dashed and solid horizontal lines indicate the $d(\text{OO})$ at which ionization and centering occur in pure ice, respectively (Ref. 12).

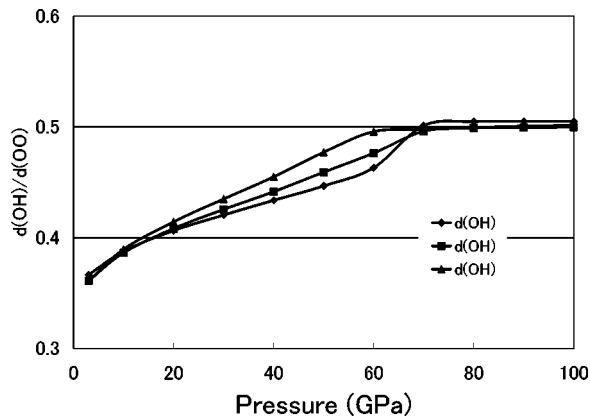


FIG. 4. Hydrogen position: The ratio $d(\text{OH})/d(\text{OO})$ calculated by density-functional theory is shown as a function of pressure.

Now, let us look into the thermal effects. Benoit *et al.*¹² recently proposed a *three-stage scenario* for explaining the hydrogen-bond centering¹³ of pure ice with increase in pressure at room temperature: under low pressure ice stays in *molecular state* where H_2O remain water molecule, then under medium pressures hydrogen atoms start to jump between two potential minima (*ionized state*), finally under high pressures hydrogen atoms move to the midpoint between the oxygen atoms (*centering state*). The $d(\text{OO})$ at which ionization and centering occur in pure ice are indicated by dashed and solid horizontal lines in Fig. 3. From this figure we can read that the ionization and centering in MH-III are expected around 40 GPa and 70 GPa, respectively. The probability distributions of $d(\text{OH})/d(\text{OO})$ for a hydrogen bond of MH-III at room temperature and with pressures 3 GPa, 40 GPa, and 80 GPa are calculated with Car-Parrinello molecular dynamics²⁶ (Fig. 5), which clearly shows that the *three-stage scenario* is also valid in MH-III but with much lower pressure than in pure ice.

Figure 6 shows the pressure dependence of normal mode frequencies of MH-III at $T=0$ K calculated with the density-functional linear-response theory.²⁷ The modes between 3000 cm^{-1} and 3500 cm^{-1} are the CH vibrations, whose frequencies monotonically increase with pressure. The modes between 2000 cm^{-1} and 3000 cm^{-1} are OH-

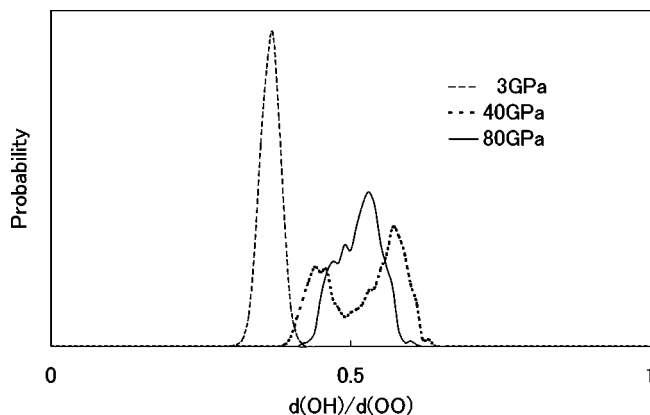


FIG. 5. Distribution of hydrogen atoms in a hydrogen bond of MH-III at 300 K.

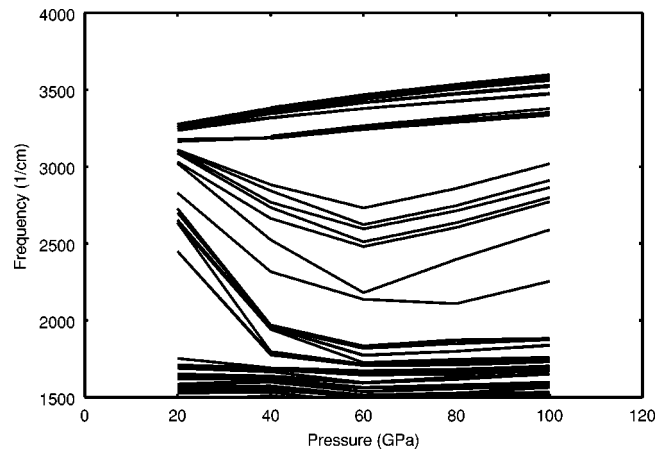


FIG. 6. Normal mode frequencies calculated with the density-functional linear-response theory as a function of pressure.

stretching modes. Their frequencies decrease monotonically up to 70 GPa, where centering occurs, and then start to increase. This tendency is qualitatively in accordance with that of pure ice.¹⁴

We calculated vibrational spectra of MH-III at 3 GPa (molecular state) for $T=300$ K and $T=30$ K as a Fourier transform of velocity-velocity correlation function obtained from Car-Parrinello molecular dynamics²⁶ and compared with the normal mode frequencies at $T=0$ K calculated with the density-functional linear-response theory.²⁷ The peak around 3100 cm^{-1} characteristic of OH-stretching vibration of hydrogen-bonded water molecules is prominent at 30 K but disappears at 300 K. This fact is consistent with the experimental observation that the Raman peak around 3100 cm^{-1} disappeared in MH-III at room temperature,⁹ and can be interpreted as the result of a strongly anharmonic potential. The disappearance of the OH-stretching Raman peak is also observed in simulations of ionized states. In vibrational spectra at 80 GPa (centering state), the OH-stretching modes of centered hydrogen bonds are located between 2000 cm^{-1} and 3000 cm^{-1} . At low temperature the peaks agrees well with the normal modes, while the peaks are blue-shifted at room temperature probably due to weak anharmonicity. The disappearance of the peak of the OH-stretching mode in molecular and ionized states at room temperature and the sur-

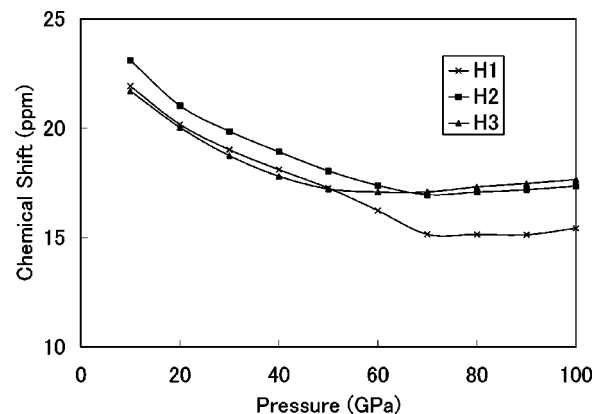


FIG. 7. ^1H -NMR chemical shift of water molecules in MH-III.

vival of the peak in centered hydrogen bond in MH-III are analogous to those in ice VII and ice X.¹⁷

We calculated also the phonon dispersion of MH-III at 80 GPa with the density-functional linear response theory.²⁷ All frequencies at all wave numbers have positive frequencies indicating the mechanical stability of this structure at zero temperature. However, further experimental and theoretical studies are necessary to prove the thermal stability at room temperature.

Figure 7 shows the ¹H-NMR chemical shift of water molecules in MH-III, which is calculated with the density-functional linear-response theory.²⁸ The result is consistent with intuitive interpretation of hydrogen-bond symmetrization. At low pressure, a proton is bound to an oxygen atom and screened by the electrons of the oxygen atom. As pressure increases, symmetrization happens and the proton moves to the midpoint between the oxygen atoms where electron density is small. Further increase in pressure makes $d(\text{OO})$ smaller and the electron density at the midpoint becomes gradually larger. Using this picture, symmetrization might be observed by ¹H-NMR when NMR measurement at such high pressure become feasible.

In summary, we studied the structural and spectral properties of high-pressure phase of methane hydrate (MH-III) with the density-functional theory, and showed that ionization and centering of hydrogen bonds in MH-III may be observed around 40 GPa and 70 GPa, respectively, which are much lower pressures than those of pure water ice (55 GPa and 100 GPa). Therefore MH-III may provide useful information about ionization and centering of hydrogen bonds between water molecules as the second example after pure ice. From the point of view of planetary science, studying physical and chemical properties of clathrate hydrates such as MH will become more and more important to interpret and to understand the information of the outer solar systems sent from space missions such as Cassini-Huygens spacecraft arriving at Saturn system in 2004.

One of the authors (T.I.) would like to thank Dr. Hiroyasu Shimizu, Dr. Shigeo Sasaki, Dr. John S. Tse, Dr. Hisako Hirai, Dr. Takashi Ikeda, Dr. Akira Hori, and Dr. Kholmurodov Kholmurzo for invaluable discussions. The results presented here were computed by using supercomputers at RIKEN and NIG.

*Electronic address: tiitaka@riken.jp

URL: <http://atlas.riken.go.jp/~tiitaka>

¹E.D. Sloan, *Clathrate Hydrates of Natural Gases* (Marcel Dekker, New York, 1998).

²J. Lunine and D. Stevenson, *Astrophys. J., Suppl.* **58**, 493 (1985).

³N. Jet Propulsion Laboratory, <http://saturn.jpl.nasa.gov/>

⁴J. Loveday, R. Nelmes, M. Guthrie, S. Belmonte, D. Allan, D. Klug, J. Tse, and Y. Handa, *Nature (London)* **410**, 661 (2001).

⁵J. Loveday, R. Nelmes, M. Guthrie, D. Klug, and J. Tse, *Phys. Rev. Lett.* **87**, 215501 (2001).

⁶I. Chou, A. Sharma, R. Burruss, R. Hemley, A. Goncharov, L. Stern, and S. Kirby, *J. Phys. Chem. A* **105**, 4664 (2001).

⁷H. Hirai, Y. Uchihara, H. Fujihisa, M. Sakashita, E. Katoh, K. Aoki, K. Nagashima, Y. Yamamoto, and T. Yagi, *J. Chem. Phys.* **115**, 7066 (2001).

⁸H. Hirai, T. Tanaka, T. Kawamura, Y. Yamamoto, and T. Yagi, *Phys. Rev. B* **68**, 172102 (2003).

⁹H. Shimizu, T. Kumazaki, T. Kume, and S. Sasaki, *J. Phys. Chem. B* **106**, 30 (2002).

¹⁰V.F. Petrenko and R.W. Whitworth, *Physics of Ice* (Oxford University Press, New York, 1999).

¹¹G.A. Jeffrey, *An Introduction to Hydrogen Bonding* (Oxford University Press, 1997).

¹²M. Benoit, A. Romero, and D. Marx, *Phys. Rev. Lett.* **89**, 145501 (2002).

¹³P. Loubeyre, R. LeToullec, E. Wolanin, M. Han, and D. Hausermann, *Nature (London)* **397**, 503 (1999).

¹⁴A. Goncharov, V. Struzhkin, H. Mao, and R. Hemley, *Phys. Rev. Lett.* **83**, 1998 (1999).

¹⁵M. Benoit, D. Marx, and M. Parrinello, *Nature (London)* **392**, 258 (1998).

¹⁶V. Struzhkin, A. Goncharov, R. Hemley, and H. Mao, *Phys. Rev. Lett.* **78**, 4446 (1997).

¹⁷K. Aoki, H. Yamawaki, M. Sakashita, and H. Fujihisa, *Phys. Rev. B* **54**, 15 673 (1996).

¹⁸K. Hirsh and W. Holzappel, *J. Chem. Phys.* **84**, 2771 (1986).

¹⁹M. Bernasconi, P. Silvestrelli, and M. Parrinello, *Phys. Rev. Lett.* **81**, 1235 (1998).

²⁰A. Putrino and M. Parrinello, *Phys. Rev. Lett.* **88**, 176401 (2002).

²¹M.C. Payne, M.P. Teter, D.C. Allan, T.A. Arias, and J.D. Joannopoulos, *Rev. Mod. Phys.* **64**, 1045 (1992).

²²D. Vanderbilt, *Phys. Rev. B* **41**, 7892 (1990).

²³J.P. Perdew, K. Burke, and M. Ernzerhof, *Phys. Rev. Lett.* **77**, 3865 (1996).

²⁴H.J. Monkhorst and J.D. Pack, *Phys. Rev. B* **13**, 5188 (1976).

²⁵G.P. Francis and M.C. Payne, *J. Phys.: Condens. Matter* **2**, 4395 (1990).

²⁶D. Marx and J. Hutter, *Modern Methods and Algorithms in Quantum Chemistry*, NIC Series Vol. 1 (Forschungszentrum, Juelich, 2000).

²⁷X. Gonze, *Phys. Rev. B* **55**, 10 337 (1997).

²⁸D. Sebastiani and M. Parrinello, *J. Phys. Chem. A* **105**, 1951 (2001).